SIN-CHN
SCIENTIFIC PRESS PTE.LTD.

Molecular & Cellular Biomechanics 2025, 22(1), 1126.
https://doi.org/10.62617/mcb1126

Article

Differentially expressed proteins of BPH with tissue inflammation based on proteomic techniques

Naiwen Zhang[1,*,†], Xinyang Yu[2,†]

[1] The Second Xiangya Hospital of Central South University, Changsha 410000, China
[2] Zhongshan College of Dalian Medical University, Dalian 116085, China
*** Corresponding author:** Naiwen Zhang, 228212259@csu.edu.cn
[†] These authors contributed equally to this work.

CITATION

Zhang N, Yu X. Differentially expressed proteins of BPH with tissue inflammation based on proteomic techniques. Molecular & Cellular Biomechanics. 2025; 22(1): 1126. https://doi.org/10.62617/mcb1126

ARTICLE INFO

Received: 16 December 2024
Accepted: 27 December 2024
Available online: 7 January 2025

Abstract: Objective: To explore the molecular mechanism of benign prostatic hyperplasia (BPH) complicated by tissue inflammation, to identify and analyze differentially expressed proteins from a proteomic perspective, and to provide a basis for elucidating the role mechanism of the inflammatory microenvironment in BPH progression and for seeking potential intervention targets. **Methods:** Sixty BPH surgical patients were included and divided into a simple BPH group (n = 30) and a BPH with tissue inflammation group (n = 30) based on histological inflammation scores. Label-free quantitative proteomic analysis was performed using liquid chromatography-tandem mass spectrometry (LC-MS/MS) to compare the expression patterns of differentially expressed proteins between the two groups. Bioinformatics tools were employed to perform functional enrichment analysis (GO, KEGG) and construct protein-protein interaction networks (STRING) for the differentially expressed proteins. Key proteins were selected and independently validated by Western blot. **Results:** A total of approximately 4900 proteins were identified. Compared with the simple BPH group, the BPH with inflammation group showed significant differences (P < 0.05, FDR < 0.05) in inflammation-related molecules (i.e., proteins primarily associated with initiating or modulating inflammatory processes; e.g., S100A8 upregulated by 3.45-fold, S100A9 upregulated by 3.22-fold, MMP9 upregulated by 3.10-fold, CCL2 upregulated by 2.98-fold) and prostate normal secretion-related proteins (e.g., MSMB downregulated to 0.12-fold, ACPP downregulated to 0.15-fold). Bioinformatic analysis showed significant enrichment of inflammation response, cell chemotaxis, ECM-receptor interaction, and Chemokine and Jak-STAT pathways. STRING analysis revealed a network distribution of key proteins, with most hub nodes concentrated in the core links of inflammation and immune regulation. Western blot validation results were consistent with the omics data, supporting the real existence and role of core proteins (i.e., proteins with high connectivity or central regulatory influence in the interaction network) in the pathological mechanism of BPH with inflammation. **Conclusion:** There are specific differentially expressed proteins in BPH with tissue inflammation, and the associated molecular networks jointly influence local microenvironment remodeling and the hyperplastic process. Elucidating the roles of these molecules and pathways helps improve our understanding of BPH pathogenesis and provides strong clues for precise diagnosis and the exploration of individualized therapeutic strategies.

Keywords: benign prostatic hyperplasia; inflammation; proteomics; differentially expressed proteins

1. Introduction

Benign prostatic hyperplasia (BPH) has a high incidence and medical burden in elderly men. During its disease progression, it is not only closely associated with lower

urinary tract symptoms but is also often accompanied by complex changes in the tissue microenvironment [1]. Previous studies have largely focused on changes in glandular structure or the screening of serum markers in hyperplasia itself, but an understanding of the intrinsic mechanisms by which local inflammation participates in this disease process remains limited [2,3]. Recent research has shown that inflammatory microenvironments can profoundly influence disease progression in various chronic conditions, including hepatic fibrosis, chronic pancreatitis, and colitis-associated colorectal carcinoma, as revealed by advanced proteomic approaches [4]. These studies highlight how inflammation-related molecules not only perpetuate tissue damage but also serve as biomarkers or therapeutic targets. In the context of the prostate, a growing number of reports indicate that inflammation accelerates hyperplasia and tissue remodeling by activating complex signaling pathways and promoting immune cell infiltration [5,6]. Incorporating examples from similar diseases underscores the promise of proteomic methods in unraveling the intricate network of inflammatory mediators and hyperplastic processes, thereby guiding more precise diagnostic and therapeutic strategies. Clinical observations and basic research continuously suggest that chronic inflammation may influence prostate enlargement and functional impairment to some extent by altering intercellular interactions, immune cell chemotaxis, and the dynamic remodeling of the extracellular matrix [7]. However, there is currently a lack of empirical evidence at the molecular level to systematically elucidate how inflammatory factors form a synergistic network with hyperplastic tissue. Traditional research methods have difficulty comprehensively capturing the fine characteristics of key protein molecular networks within the tissue and have not precisely described the complex interactions of potential signaling pathways [8,9]. Employing high-throughput, systematic proteomic technologies to analyze the differentially expressed proteins in BPH tissues coexisting with inflammation from a holistic perspective is expected to fill this gap, providing objective evidence for understanding newly emerged key molecules and signaling axes during the hyperplastic process, and laying a foundation for finding new approaches to diagnosis and treatment [10]. In this study, proteomic technologies were utilized to comparatively analyze the protein expression profiles of benign prostatic hyperplasia tissues with and without local inflammation, and, combined with functional enrichment and interaction network analyses, to elucidate the relevant molecular mechanisms and potential regulatory links. The aim of this research is to reveal the influence patterns of key molecules in the inflammatory microenvironment on the hyperplastic process, thus offering novel and precise references for subsequent selection of molecular markers and for the design of individualized treatment strategies.

2. Materials and methods

2.1. Study period and ethical approval

This study was conducted from July 2022 to July 2024 in the Department of Urology at The Second Xiangya Hospital of Central South University. The study protocol was approved by the hospital's Medical Ethics Committee (approval number: 2022137). All participants provided written informed consent.

2.2. Study subjects and sample collection

A total of 60 subjects with benign prostatic hyperplasia (BPH) scheduled for surgical treatment were included. Inclusion criteria: (1) Clinically and radiologically confirmed diagnosis of BPH; (2) Age between 60 and 80 years; (3) No pharmacological or physical interventions that could influence molecular expression in prostate tissue within the past 3 months. Exclusion criteria: (1) Histopathological examination confirming prostate cancer or other urogenital malignancies; (2) Severe cardiac insufficiency, cirrhosis, or chronic renal insufficiency; (3) Evidence of acute urinary tract infection within 2 weeks (including imaging and laboratory findings).

Immediately after surgery, approximately 0.5 cm^3 of prostate tissue was excised, rapidly frozen in liquid nitrogen, and transferred to an −80 ℃ ultra-low temperature freezer for storage to ensure sample quality for subsequent proteomic analyses.

2.3. Histology and inflammation assessment

Prostate tissue stored at −80 ℃ was fixed in 4% paraformaldehyde for 24 h, followed by routine histological processing, including gradient ethanol dehydration, paraffin embedding, and preparation of 5 μm-thick continuous sections. The sections were stained with hematoxylin-eosin (H&E). Two independent pathologists evaluated the degree of inflammatory cell infiltration under double-blind conditions based on an inflammation scoring system: 0 points indicated no obvious inflammatory cell infiltration, 1 point indicated mild infiltration, 2 points indicated moderate infiltration, and 3 points indicated severe infiltration [11]. Subjects with an inflammation score ≥ 1 were defined as the BPH with tissue inflammation group (30 cases), and those with a score of 0 were defined as the simple BPH group (30 cases).

2.4. Protein extraction and quantification

Take the tissue sample (approximately 50 mg) out from −80 ℃ storage and grind it into powder under liquid nitrogen conditions. Place the powder into a lysis solution containing 50 mM Tris-HCl (pH 8.0), 8 M urea, 1 mM PMSF, and 1 × protease inhibitor (Roche Diagnostics). Lyse using a Scientz-IID ultrasonic disruptor in an ice bath (power 200 W, sonication for 2 s, interval 2 s, repeated 30 times). Centrifuge at 12,000 × g (4 ℃) for 10 min to collect the supernatant as the total protein extract. Use the Pierce BCA Protein Assay Kit (Thermo Fisher Scientific) to quantify the protein concentration according to the standard curve, and adjust the protein concentration to approximately 2 μg/μL.

2.5. Protein digestion and peptide preparation

Weigh 100 μg of protein from each sample and add 5 mM DTT. Heat at 56 ℃ in a water bath for 30 min to reduce the protein disulfide bonds. After cooling, add 20 mM iodoacetamide (IAA) and incubate at room temperature in the dark for 30 min to complete alkylation. Add 100 mM NH_4HCO_3 solution to reduce the urea concentration to below 1 M. Add trypsin (Promega) at an enzyme-to-substrate mass ratio of 1:50 and incubate at 37 ℃ for 16 h for digestion. Purify the digestion products using a C18 solid-phase extraction cartridge (Waters) and lyophilize using a Labconco freeze-dryer for later use [12].

2.6. Liquid chromatography-tandem mass spectrometry (LC-MS/MS) analysis

Dissolve the lyophilized peptides in 0.1% formic acid solution. Use a Thermo Dionex UltiMate 3000 nano LC system to load the samples onto a PepMap C18 nano column (75 μm × 25 cm, 2 μm particle size, Thermo Fisher Scientific). Mobile phase A is 0.1% formic acid in water, and mobile phase B is 80% acetonitrile with 0.1% formic acid in water. The gradient elution program is as follows: 0–5 min hold at 5% B, 5–45 min increase linearly from 5% B to 30% B, 45–55 min increase from 30% B to 45% B, 55–60 min increase from 45% B to 80% B, and 60–65 min maintain at 80% B. The flow rate is 300 nL/min.

The separated peptides enter a Q Exactive HF mass spectrometer (Thermo Fisher Scientific) with a mass range of m/z 350–1800 in positive ion mode. Full scan resolution is set to 120,000, and the top 20 most abundant ions are selected for HCD secondary mass spectrometry analysis (collision energy set to 28%) [13]. The dynamic exclusion time is set to 30 s to reduce repeated scans.

2.7. Data processing and differentially expressed protein screening

Use MaxQuant software to analyze the raw mass spectrometry data, with the UniProt human protein database (search date: August 2023) as the search database. Peptide matching error is less than 10 ppm, and the FDR for the first- and second-level mass spectra is controlled within 1%. Each protein is required to have at least 1 unique peptide. The LFQ (Label-Free Quantification) method is used to compare protein expression levels between the two groups of samples. An independent sample *t*-test is conducted to assess the significance of differences, with $P < 0.05$ considered significant. A Fold Change ≥ 1.5 or ≤ 0.67 is considered biologically significant. Statistical analysis is performed using SPSS 26.0 software.

2.8. Bioinformatics analysis

Use the DAVID and STRING databases to perform Gene Ontology functional analysis and KEGG pathway enrichment analysis on the screened differentially expressed proteins. Focus on functional items and pathways related to inflammatory signal transduction, immune cell chemotaxis, cell proliferation, and extracellular matrix remodeling. $P < 0.05$ is considered the criterion for significant enrichment.

2.9. Verification of differential proteins

Select 3 to 5 differentially expressed proteins highly related to inflammation and the hyperplasia process for Western blot verification. Repeat the above protein extraction operations in 8 independent BPH with tissue inflammation group samples and 8 simple BPH group samples. Take 20 μg of total protein from each sample, separate it by 10% SDS-PAGE electrophoresis (voltage 100 V, electrophoresis about 60 min), then transfer to a PVDF membrane (Millipore). After blocking with 5% skim milk solution at room temperature for 1 h, add the specific primary antibody (Cell Signaling Technology, 1:1000 dilution) and incubate at 4 ℃ overnight. After washing the membrane, add the HRP-labeled secondary antibody (Cell Signaling Technology, 1:5000 dilution) and incubate at room temperature for 1 h. Develop with ECL reagent

(Thermo Fisher Scientific), photograph using a Bio-Rad Chemidoc Touch imaging system, and perform grayscale value quantification using ImageJ software. ACTB (*β*-Actin) is used as an internal control for data normalization. Differences in grayscale values between groups are evaluated by an independent sample *t*-test, with $P < 0.05$ considered significant.

2.10. Statistical analysis

All continuous variables are expressed as mean ± standard deviation. An independent sample *t*-test is used for comparisons between the two groups to determine the significance of differences ($P < 0.05$ is considered significant) with SPSS 26.0 software. During the protein screening stage of multiple comparisons, the Benjamini-Hochberg method is used to control the FDR within 1% to ensure the robustness of the results.

2.11. Reproducibility and quality control

Three biological replicates are set for each group of samples to ensure data stability. Before mass spectrometry analysis, a known standard protein mixture is used to calibrate the instrument's sensitivity and resolution, and blank controls are included in each batch to monitor background signals. During data processing, low-quality spectra and noise peaks are strictly excluded to ensure the reliability and reproducibility of the final identification results.

3. Results

3.1. Clinical and pathological characteristics

Compared with the simple BPH group, the BPH with tissue inflammation group showed significantly higher prostate volume, symptom scores, and inflammation scores ($P < 0.05$). No statistically significant differences were observed in age or PSA levels ($P > 0.05$). These results indicate certain significant differences between the two groups (**Table 1**).

Table 1. Comparison of clinical and pathological characteristics of subjects.

Indicator	Simple BPH Group ($n = 30$)	BPH with Tissue Inflammation Group ($n = 30$)	*t*-value	*P*-value
Age (years)	68.70 ± 4.32	69.20 ± 3.88	0.560	0.578
Prostate Volume (mL)	55.00 ± 6.00	63.00 ± 7.50	2.570	0.013*
Serum PSA Level (ng/mL)	2.90 ± 0.40	3.10 ± 0.45	1.105	0.273
International Prostate Symptom Score (IPSS)	18.20 ± 2.45	20.50 ± 2.80	2.110	0.041*
Inflammation Score (0–3 points)	0.00 ± 0.00	1.80 ± 0.25	25.603	< 0.001*

Note: * indicates $P < 0.05$, representing statistical significance.

3.2. Proteomic identification and screening of differentially expressed proteins

While obtaining a large number of high-confidence identified proteins, the techniques and biological replicates used in this study both exhibited high consistency,

ensuring the accuracy and coverage of the identification of differential proteins and effectively controlling the FDR within a reasonable range (**Table 2**). Statistical analysis results showed that most proteins did not exhibit significant changes, with only a small number of proteins showing significant upregulation or downregulation ($P < 0.05$), clearly distributed on both sides of the plot. Some key molecules (such as S100A8, MSMB) have been indicated in the corresponding figures (**Figure 1A**), laying the foundation for subsequent mechanistic exploration. Further screening of the differential proteins based on Fold Change and *P*-values identified the 20 most representative upregulated and 20 most representative downregulated proteins, listed in a table. After FDR correction, all showed statistically significant differences ($P < 0.05$) (**Table 3**). In addition, through cluster analysis, it could be observed that the significantly differentially expressed proteins formed distinct expression pattern clusters in the heatmap (**Figure 1B**). Samples in the BPH with tissue inflammation group showed higher standardized relative expression levels (redder color) for some proteins, while the simple BPH group tended towards neutral or bluer distributions. Clustering by rows grouped proteins with similar functional characteristics into adjacent branches, and clustering by columns clearly differentiated the two groups of samples, providing a clear molecular profile from an overall perspective for further pathological mechanism studies.

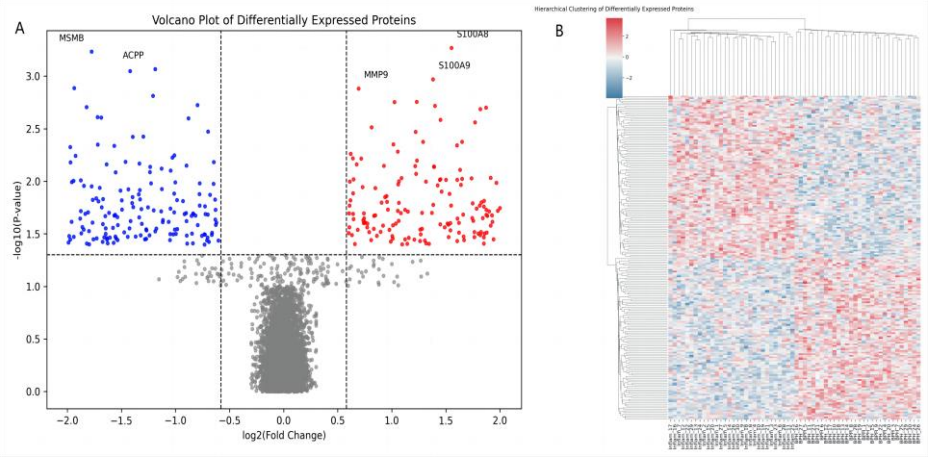

Figure 1. Global analysis of differentially expressed proteins: **(A)** Volcano plot of differentially expressed proteins; **(B)** Hierarchical clustering heatmap of differentially expressed proteins.

Table 2. Total number of identified and quantified proteins and quality control indicators.

Indicator	Overall Statistical Indicators for Simple BPH Group	Overall Statistical Indicators for BPH with Tissue Inflammation Group
Total number of identified proteins	4853.46 ± 212.57	4974.88 ± 228.13
Average number of peptides (per protein)	8.63 ± 1.14	9.08 ± 1.27
Average peptide coverage (%)	22.73 ± 2.07	23.96 ± 2.09
Protein and peptide level FDR (%)	Protein: 0.82 ± 0.09; Peptide: 0.96 ± 0.13	Protein: 0.79 ± 0.07; Peptide: 0.91 ± 0.14
Pearson correlation coefficient between technical replicates (mean ± SD)	0.93 ± 0.02	0.94 ± 0.03
Pearson correlation coefficient between biological replicates (mean ± SD)	0.91 ± 0.04	0.89 ± 0.03

Table 3. Lists of the top 20 significantly upregulated and top 20 downregulated proteins.

Protein Name (Gene Symbol)	Fold Change	*P*-value	Adjusted *P*-value (*q*-value)
Upregulated Proteins			
S100A8	3.45	< 0.001	0.001
S100A9	3.22	0.001	0.002
MMP9	3.10	0.002	0.003
CCL2	2.98	0.003	0.005
IL1RN	2.83	0.005	0.007
CXCL8	2.75	0.006	0.009
PTX3	2.63	0.008	0.012
SERPINE1	2.58	0.01	0.015
MMP12	2.5	0.012	0.018
TNF	2.44	0.015	0.021
IL6R	2.35	0.018	0.025
ICAM1	2.29	0.022	0.029
PLAU	2.18	0.025	0.030
TLR2	2.09	0.028	0.033
CD14	2	0.031	0.035
CSF3	1.94	0.034	0.038
CXCL1	1.88	0.037	0.04
CXCL10	1.82	0.039	0.042
HMGB1	1.75	0.041	0.044
CXCL2	1.66	0.044	0.046
Downregulated Proteins			
MSMB	0.12	< 0.001	0.001
ACPP	0.15	0.001	0.002
SEMG1	0.18	0.002	0.003
SEMG2	0.22	0.003	0.005
KLK3	0.25	0.005	0.007
KRT8	0.28	0.006	0.009
DSP	0.31	0.008	0.012
KRT18	0.33	0.01	0.015
KLK2	0.37	0.012	0.018
NPPA	0.39	0.015	0.021
SCGB3A1	0.41	0.018	0.025
KLK4	0.44	0.021	0.029
TGM4	0.47	0.023	0.030
KLK11	0.5	0.026	0.033
SERPINA3	0.53	0.029	0.035
SPON2	0.56	0.032	0.038
PSAP	0.59	0.034	0.04
CGA	0.61	0.036	0.042
CFAP65	0.63	0.038	0.044
TFF3	0.65	0.041	0.046

3.3. Bioinformatics analysis and functional interpretation

Among the functional areas involved in the differential proteins, inflammatory response, cell chemotaxis, and extracellular matrix-related processes all showed significant enrichment ($P < 0.05$, FDR < 0.05), and multiple signaling pathways (such as ECM-receptor, chemokine, and Jak-STAT pathways) were clearly represented (**Table 4**), providing strong clues for further in-depth molecular mechanism research. Further use of STRING interaction analysis to construct a high-confidence network revealed that upregulated and downregulated proteins exhibited obvious differentiation in a scale-free, force-directed layout (**Figure 2**). Through connections with STRING scores ≥ 0.7, the network displayed synergistic interactions among the related molecules. Most key nodes were located at the network's core, facilitating an understanding of their potential functional relationships from a global perspective.

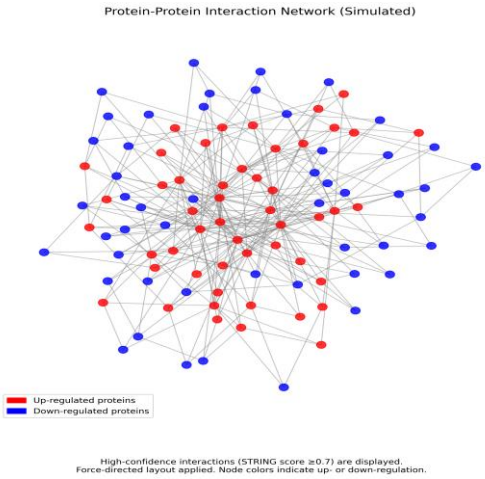

Figure 2. Interaction network diagram of differential proteins based on STRING database analysis.

Table 4. GO and KEGG functional enrichment analysis results of differentially expressed proteins.

Functional Item Name	Category	Number of Differential Proteins Involved	*P*-value	FDR	Enrichment Fold
Inflammatory response	Biological Process (BP)	18	< 0.001	0.002*	3.45
Leukocyte chemotaxis	Biological Process (BP)	12	0.001	0.005*	2.91
Response to cytokine stimulus	Biological Process (BP)	22	0.003	0.007*	2.05
Extracellular matrix organization	Biological Process (BP)	9	0.002	0.006*	3.12
Cell-cell adhesion	Biological Process (BP)	15	0.005	0.010*	1.89
Proteinaceous extracellular matrix	Cellular Component (CC)	7	0.010	0.014*	2.63
Chemokine activity	Molecular Function (MF)	5	0.004	0.009*	3.77
Oxidoreductase activity	Molecular Function (MF)	11	0.008	0.013*	1.72
ECM-receptor interaction	KEGG Pathway (KEGG)	19	< 0.001	0.001*	4
Chemokine signaling pathway	KEGG Pathway (KEGG)	14	0.002	0.005*	2.54
Jak-STAT signaling pathway	KEGG Pathway (KEGG)	20	0.006	0.011*	2.38
MAPK signaling pathway	KEGG Pathway (KEGG)	13	0.003	0.008*	2.46

Note: * indicates P < 0.05, representing statistical significance.

3.4. Verification of key differential proteins

By conducting independent sample *t*-tests, the expression differences of the selected target proteins between the two groups all reached statistical significance ($P < 0.05$). The relative optical density values showed an overall increase in the upregulated proteins in the BPH with inflammation group, while the downregulated proteins were significantly reduced (**Figure 3**). The error bars and *P*-value markings in the bar charts reflected the robustness and credibility of the results. This verification result echoed the proteomic data, providing further support for the findings.

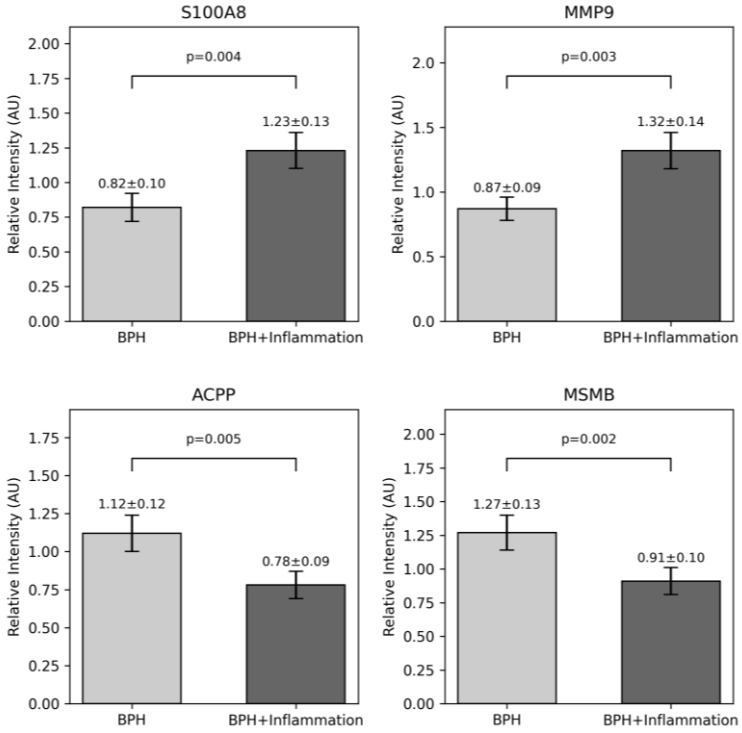

Figure 3. Western blot verification results of differentially expressed proteins.

4. Discussion

The observed changes in protein expression patterns in this study point to a special microenvironment formed under conditions of local inflammation coexisting with benign prostatic hyperplasia (BPH). In this state, inflammatory-related molecules represented by S100A8, S100A9, CCL2, IL1RN, TNF, and several chemokines exhibit significantly increased expression levels, while proteins associated with normal prostate tissue structure and secretory function are markedly decreased. Specifically, S100A8 and S100A9 (often collectively referred to as calprotectin) can bind to receptors such as Toll-like receptor 4 (TLR4) and the receptor for advanced glycation end-products (RAGE), thereby enhancing the activation of the NF-κB pathway and amplifying local inflammatory signals [14,15]. Meanwhile, these proteins actively recruit and stimulate neutrophils or macrophages, further exacerbating tissue inflammation and remodeling. During this process, MMP9, a key member of the matrix metalloproteinase family, not only degrades the extracellular matrix (ECM) to create a permissive environment for cellular proliferation and migration but also contributes to the activation of various inflammatory mediators and growth factors, ultimately

promoting tissue remodeling and fibromuscular hyperplasia [16]. In the inflammatory microenvironment of BPH, the sustained overexpression of MMP9 may accelerate structural disorganization and facilitate a positive feedback loop between inflammation and hyperplasia, jointly driving the progression of BPH. This expression pattern is not an isolated phenomenon; rather, it provides vivid examples for understanding the underlying molecular dynamics of the lesion [17]. Chronic local inflammation may play a promoting role in the process of prostatic hyperplasia. Its impact is not limited to individual molecules but changes local intercellular communication methods through the entire signaling network [18]. In this state, immune cells are more easily attracted and aggregate, while cell adhesion, signal transduction, and tissue metabolic activities are gradually remodeled, making interactions between epithelial and stromal cells more complex. As the diversity of local signals increases, the physical attributes and chemical environment of the microstructure also continue to evolve, closely relating to glandular duct narrowing and enlarged hyperplastic tissues [19]. From this perspective, inflammation is not merely a tissue pathological phenomenon but also a driving factor that promotes the hyperplastic process. Inflammation-driven molecules may enhance the tendency toward hyperplasia by promoting fibroblast proliferation, the release of secretory factors, and matrix remodeling, thereby interfering with the normal physiological functioning of the prostate [20]. This combined effect on structure and function makes BPH, when coexisting with inflammation, present more complex clinical characteristics, not only manifesting more pronounced symptoms but also showing greater variability in response to interventions. In addition, the significant differences in prostate volume and inflammation scores observed between the two groups likely contributed to the distinct protein expression profiles. The synergy of increased glandular size and heightened inflammatory infiltration may amplify the production of pro-inflammatory mediators and accelerate extracellular matrix remodeling, creating a microenvironment more prone to hyperplasia. Thus, baseline discrepancies in anatomical and inflammatory status should be carefully considered when interpreting proteomic changes, as they can influence both the magnitude and direction of protein dysregulation. Recognizing these baseline factors helps strengthen the reliability of our conclusions, emphasizing the need for stratifying patient samples or adjusting statistical models to account for such variability in future research and clinical applications. These findings provide solid molecular evidence for understanding the pathogenesis of BPH and imply that early intervention in inflammation-related signaling pathways may achieve results in reducing gland enlargement, alleviating symptoms, and slowing progression. Further research could include these key molecules in the screening range of potential diagnostic and therapeutic strategies, approaching from the perspective of molecular typing and precise intervention, thereby creating conditions for improving the scientific and targeted nature of treatment decisions.

In the early stages, glandular tissue hyperplasia is often regarded merely as a disordered structural expansion. However, as molecular-level evidence continues to accumulate, it becomes clear that the profound changes in the local microenvironment are not limited to the cellular level. When many molecules associated with extracellular matrix organization, degradation, and remodeling exhibit significant

distribution shifts, the surrounding tissue environment correspondingly alters its physical and chemical properties, thereby influencing the hyperplastic process and clinical symptom presentation [21]. The stromal region of the gland plays a key role in this dynamic regulation. The balance between certain proteases and their related inhibitors becomes skewed, causing the composition and arrangement of the extracellular matrix to become unstable [22]. Accompanying these changes, cell adhesion, signal transduction, and the modes of matrix-cell interaction no longer follow normal physiological trajectories. Potential mechanical stresses and molecular signals within the microenvironment guide subtle changes in the behavioral patterns of local cell communities. Even minimal but sustained remodeling may increase the tissue's plasticity, thereby providing proliferating cells with more space and pathways to expand, and offering infiltrating immune cells more opportunities for attachment and migration, ultimately forming a continuous and recurrent cycle. As the volume of hyperplastic tissue continues to grow, the normal ductal structure and secretory function are gradually restricted, potentially manifesting as more pronounced clinical symptoms [23]. These are not merely additive pathological processes but rather feedback results that reinforce each other within a dynamic network. Such a process reflects a full-range cascade effect from molecules to tissues and then to function. Recognizing this significance at the matrix level allows for the opportunity to seek therapeutic strategies starting from matrix intervention—whether by blocking the activity of specific matrix-degrading enzymes, correcting the disorder of adhesion molecules, or maintaining ECM balance. Such interventions may influence the rate of gland progression, alleviate patient symptoms, and improve the effectiveness of treatment. This perspective suggests that focusing solely on cellular hyperplasia is insufficient; instead, starting from the regulation of the microenvironment provides a basis for developing more precise and personalized intervention methods for different types of patients.

Those molecules located at the core of the interaction network no longer merely reflect differences in a single specific pathway; rather, they serve as hubs coordinating the operation of multiple signaling pathways. When chemokines and inflammation-related proteins act in concert, the positioning and activation of local immune cells are no longer random events. Instead, the tissue microenvironment can modulate the intensity of immune responses through precisely regulated signal gradients [24]. In this state, intercellular information exchange is not characterized by one-way instructions from a particular cell type, but rather by a sophisticated network formed through mutual influences among various molecules. Against this backdrop, immune cells distribute and migrate in a more orderly manner, guided by chemotactic signals that provide direction, while critical intracellular pathways regulate their response rate and quality [25]. The synchronized enrichment of multiple signaling pathways offers a stable framework for this complex process, such that immune system activity no longer exists in isolation but is integrated into a dynamic and sensitive regulatory network. This configuration helps explain the variability and rapid progression of the hyperplastic process under inflammatory conditions: once immune cells are effectively organized, persistent local stimuli and cellular secreted factors continuously strengthen the feedback loops, enabling hyperplasia and inflammation to mutually enhance each other at the molecular level [26]. Furthermore, a broader

systems biology perspective is warranted to fully appreciate how the enriched GO terms and KEGG pathways interact and reinforce one another in the context of BPH with inflammation. Although our findings highlight the involvement of chemokine signaling, ECM-receptor interactions, and Jak-STAT pathways, these are not isolated mechanisms. Instead, they likely converge at multiple regulatory nodes, creating a dynamic network in which inflammatory mediators, immune cell recruitment, and matrix remodeling perpetuate one another. By extending beyond pathway listing to include network analyses—such as co-expression modules or hub-gene identification—future investigations can pinpoint critical bottlenecks or central hubs where therapeutic interventions may exert maximum impact. This holistic approach could uncover synergistic relationships among pathways, offering a more comprehensive framework for understanding BPH pathogenesis and identifying novel, more effective intervention strategies. Such networked regulatory mechanisms provide insights for the design of future intervention strategies, where selecting specific nodes or pathways for blockade could significantly influence the entire system's response, laying the foundation for optimizing potential therapeutic strategies.

After obtaining accurate and stable proteomic results, further independent sample verification confirmed that the abnormal expression of key molecules was not a technical coincidence. The specific biological processes and signaling pathways reflected by these molecules may have potential diagnostic and prognostic value at the individual level. Emphasizing the pathological mechanisms associated with these specific molecules helps to summarize appropriate early detection indicators at the molecular level, providing more accurate data support for clinical decision-making. Whereas previous diagnostic models often relied on generalized judgments from imaging or serum markers, it is now possible to consider including these molecules in classification strategies. By distinguishing between inflammatory-driven hyperplastic patterns and relatively simple hyperplastic morphologies based on their expression levels, we can guide therapeutic interventions. On the intervention front, treatment is not limited to traditional surgery or symptomatic therapies. Instead, it becomes feasible to design precise intervention plans centered on specific molecules. If some inflammation-driven proteins play pivotal roles in regulating BPH progression, inhibiting them may reduce the lesion's attractiveness to immune infiltration and disrupt the persistent stimulatory feedback loops. Meanwhile, inhibiting ECM-degrading factors or regulating particular signaling axes may slow hyperplastic expansion while maintaining basic glandular structure and function, thereby creating more favorable conditions for symptom improvement. Through these new approaches, clinical practice can integrate molecular classification, targeted blockade, and individualized treatment, thereby enhancing the effectiveness of interventions and yielding more significant benefits for patients.

From a translational perspective, these differentially expressed proteins hold promise as potential diagnostic and therapeutic targets. For instance, elevated S100A8 and S100A9 levels could function as early indicators of an inflammation-driven hyperplastic process, helping to distinguish between simple BPH and inflammation-associated hyperplasia. Furthermore, strategies aimed at inhibiting MMP9 activity may be beneficial in halting the extracellular matrix remodeling cycle that contributes to disease progression. By integrating these markers into clinical decision-making,

clinicians could tailor interventions and stratify patients based on the intensity of inflammatory and matrix-altering signals. This approach may not only improve diagnostic accuracy but also pave the way for personalized therapies that target the underlying molecular mechanisms, thereby enhancing both treatment efficacy and patient quality of life. These findings have important implications for personalized medicine and early diagnosis in BPH. Identifying and quantifying inflammation-driven proteins can guide clinicians in stratifying patients based on their underlying inflammatory burden, allowing for more targeted therapeutic decisions. For instance, patients with pronounced upregulation of S100A8, S100A9, or MMP9 could benefit from early anti-inflammatory interventions or ECM-targeting agents aimed at halting disease progression. Moreover, the distinct expression patterns revealed by our proteomic analysis could serve as the basis for developing noninvasive biomarker panels that detect subtle shifts in the local inflammatory environment before overt clinical symptoms arise. By incorporating these molecular insights into routine clinical practice, practitioners may be able to differentiate between simple hyperplasia and inflammation-associated BPH, optimize therapeutic regimens, and monitor treatment responses more accurately, ultimately improving long-term patient outcomes.

5. Conclusion

From a proteomic perspective, this study has clearly identified the key molecules and pathways associated with inflammation in BPH. These molecules not only map out microenvironmental remodeling and tissue structural variations driven by local inflammation but also indicate potential regulatory hubs and therapeutic targets. With dynamic changes in the stroma and coordinated immune networks, the hyperplastic process at the molecular level exhibits distinct functional differentiation characteristics. In this way, these molecular findings can be fully utilized in precise diagnosis and personalized treatment strategies, thereby optimizing clinical decision-making and improving the scientific and effective management of patients.

Author contributions: Conceptualization, NZ and XY; methodology, NZ and XY; formal analysis, NZ and XY; investigation, NZ and XY; writing—original draft preparation, NZ and XY; writing—review and editing, NZ and XY; project administration, NZ and XY. All authors have read and agreed to the published version of the manuscript.

Ethical approval: Not applicable.

Conflict of interest: The authors declare no conflict of interest.

References

1. Xiang, P., Liu, D., Guan, D., Du, Z., Hao, Y., Yan, W., Wang, M., & Ping, H. (2021). Identification of key genes in benign prostatic hyperplasia using bioinformatics analysis. World Journal of Urology, 39, 3509–3516. https://doi.org/10.1007/s00345-021-03625-5.
2. Bellei, E., Caramaschi, S., Giannico, G., Monari, E., Martorana, E., Bonetti, R., & Bergamini, S. (2023). Research of Prostate Cancer Urinary Diagnostic Biomarkers by Proteomics: The Noteworthy Influence of Inflammation. Diagnostics, 13. https://doi.org/10.3390/diagnostics13071318.
3. Sachdeva, R., Kaur, N., Kapoor, P., Singla, P., Thakur, N., & Singhmar, S. (2022). Computational analysis of protein-protein

interaction network of differentially expressed genes in benign prostatic hyperplasia. Molecular Biology Research Communications, 11, 85–96. https://doi.org/10.22099/mbrc.2022.43721.1746.

4. Ke, Z., Cai, H., Wu, Y., Lin, Y., Li, X., Huang, J., Sun, X., Zheng, Q., Xue, X., Wei, Y., & Xu, N. (2019). Identification of key genes and pathways in benign prostatic hyperplasia. Journal of Cellular Physiology, 234, 19942–19950. https://doi.org/10.1002/jcp.28592.
5. Hao, L., Thomas, S., Greer, T., Vezina, C., Bajpai, S., Ashok, A., De Marzo, A., Bieberich, C., Li, L., & Ricke, W. (2019). Quantitative proteomic analysis of a genetically induced prostate inflammation mouse model via custom 4-plex DiLeu isobaric labeling. American journal of physiology. Renal physiology, 316 6, F1236-F1243 . https://doi.org/10.1152/ajprenal.00387.2018.
6. Lin, D., & Chen, Z. (2022). PD16-03INVOLVEMENT OF YES-ASSOCIATED PROTEIN 1 IN INFLAMMATION-INDUCED BENIGN PROSTATIC HYPERPLASIA. The Journal of Urology, 207, e270. https://doi.org/10.1097/JU.0000000000002548.03.
7. Gao, Z., Zhao, Y., Wang, J., Wu, Z., Lu, G., Wu, Q., Wang, Y., & Yu, H. (2023). Mechanisms Research on Benign Prostatic Hyperplasia Intervened by Tong Guan Pill Based on Label Free Proteomics. 2023 IEEE International Conference on Bioinformatics and Biomedicine (BIBM), 4561-4568. https://doi.org/10.1109/BIBM58861.2023.10385597.
8. Lo, H., Yu, D., Gao, H., Tsai, M., & Chuang, E. (2020). IL-27/IL-27RA signaling may modulate inflammation and progression of benign prostatic hyperplasia via suppressing the LPS/TLR4 pathway. Translational Cancer Research, 9, 4618–4634. https://doi.org/10.21037/tcr-20-1509.
9. Reyes, N., Tiwari, R., & Geliebter, J. (2020). Abstract 5591: Differential profiles of pro-inflammatory chemokines identified in patients with prostate cancer and benign prostatic hyperplasia. Immunology. https://doi.org/10.1158/1538-7445.am2020-5591.
10. Barashi, N., Li, T., Angappulige, D., Zhang, B., O'Gorman, H., Nottingham, C., Shetty, A., Ippolito, J., Andriole, G., Mahajan, N., Kim, E., & Mahajan, K. (2024). Symptomatic Benign Prostatic Hyperplasia with Suppressed Epigenetic Regulator HOXB13 Shows a Lower Incidence of Prostate Cancer Development. Cancers, 16. https://doi.org/10.3390/cancers16010213.
11. Li, Y., Liu, J., Liu, D., Wang, Z., Zhou, Y., Yang, S., Guo, F., Yang, L., & Zhang, X. (2022). The Prostate-Associated Gene 4 (PAGE4) Could Play a Role in the Development of Benign Prostatic Hyperplasia under Oxidative Stress. Oxidative Medicine and Cellular Longevity, 2022. https://doi.org/10.1155/2022/7041739.
12. Ploypetch, S., Wongbandue, G., Roytrakul, S., Phaonakrop, N., & Prapaiwan, N. (2023). Comparative Serum Proteome Profiling of Canine Benign Prostatic Hyperplasia before and after Castration. Animals: An Open Access Journal from MDPI, 13. https://doi.org/10.3390/ani13243853.
13. Unno, R., Akutagawa, J., Song, H., Hui, K., Chen, Y., Pham, J., Yang, H., Huang, F., & Chi, T. (2023). Single cell transcriptional profiling of benign prostatic hyperplasia reveals a progenitor-like luminal epithelial cell state within an inflammatory microenvironment. bioRxiv. https://doi.org/10.1101/2023.11.06.565375.
14. Sivoňová, K., Tatarkova, Z., Jurečeková, J., Kliment, J., Híveš, M., Lichardusová, L., & Kaplan, P. (2020). Differential profiling of prostate tumors versus benign prostatic tissues by using a 2DE-MALDI-TOF-based proteomic approach. Neoplasma. https://doi.org/10.4149/neo_2020_200611N625.
15. Correll, V., Otto, J., Risi, C., Main, B., Boutros, P., Kislinger, T., Galkin, V., Nyalwidhe, J., Semmes, O., & Yang, L. (2022). Optimization of small extracellular vesicle isolation from expressed prostatic secretions in urine for in-depth proteomic analysis. Journal of Extracellular Vesicles, 11. https://doi.org/10.1002/jev2.12184.
16. Xiao, H., Jiang, Y., He, W., Xu, D., Chen, P., Liu, D., Liu, J., Wang, X., DiSanto, M., & Zhang, X. (2020). Identification and functional activity of matrix-remodeling associated 5 (MXRA5) in benign hyperplastic prostate. Aging (Albany NY), 12, 8605 - 8621. https://doi.org/10.18632/aging.103175.
17. Pascal, L., Mizoguchi, S., Chen, W., Rigatti, L., Igarashi, T., Dhir, R., Tyagi, P., Wu, Z., Yang, Z., De Groat, W., DeFranco, D., Yoshimura, N., & Wang, Z. (2021). Prostate-Specific Deletion of Cdh1 Induces Murine Prostatic Inflammation and Bladder Overactivity. Endocrinology, 162 1. https://doi.org/10.1210/endocr/bqaa212.
18. Kawahara, R., Recuero, S., Nogueira, F., Domont, G., Leite, K., Srougi, M., Thaysen-Andersen, M., & Palmisano, G. (2019). Tissue Proteome Signatures Associated with Five Grades of Prostate Cancer and Benign Prostatic Hyperplasia. PROTEOMICS, 19. https://doi.org/10.1002/pmic.201900174.
19. Middleton, L., Shen, Z., Varma, S., Pollack, A., Gong, X., Zhu, S., Zhu, C., Foley, J., Vennam, S., Sweeney, R., Tu, K.,

Biscocho, J., Eminaga, O., Nolley, R., Tibshirani, R., Brooks, J., West, R., & Pollack, J. (2019). Genomic analysis of benign prostatic hyperplasia implicates cellular re-landscaping in disease pathogenesis. JCI insight, 5. https://doi.org/10.1172/jci.insight.129749.

20. Huan Xie,Junli Fan,Jiajun Wang,Tao Liu,Lili Chen,Yunbao Pan... & Xinran Li. (2024). Serological proteomic profiling uncovered CDK5RAP2 as a novel marker in benign prostatic hyperplasia. Clinical biochemistry 110867.
21. Latosinska, A., Davalieva, K., Makridakis, M., Mullen, W., Schanstra, J., Vlahou, A., Mischak, H., & Frantzi, M. (2020). Molecular Changes in Tissue Proteome during Prostate Cancer Development: Proof-of-Principle Investigation. Diagnostics, 10. https://doi.org/10.3390/diagnostics10090655.
22. Yan Cui, Hui Wang & Yuting Wang. (2024). Plasma metabolites as mediators in the relationship between inflammation-related proteins and benign prostatic hyperplasia: insights from mendelian randomization. Scientific Reports (1), 26152-26152.
23. Junya Hata,Kanako Matsuoka,Yuki Harigane,Kei Yaginuma,Hidenori Akaihata,Satoru Meguro... & Yoshiyuki Kojima. (2024). Proliferative mechanism of benign prostatic hyperplasia by NLRP3 inflammasome through the complement pathway. International journal of urology: official journal of the Japanese Urological Association (12), 1429-1437.
24. Lei Xu, Yi Xu, Shouzhen Chen & Benkang Shi. (2024). A comprehensive analysis and comparison of lipid metabolism and inflammatory indices in patients with benign prostatic hyperplasia and prostate cancer. Holistic Integrative Oncology (1), 37–37.
25. Fernanda Caramella Pereira,Qizhi Zheng,Jessica L Hicks,Sujayita Roy,Tracy Jones,Martin Pomper... & W Nathaniel Brennen. (2024). Overexpression of Fibroblast Activation Protein (FAP) in stroma of proliferative inflammatory atrophy (PIA) and primary adenocarcinoma of the prostate. medRxiv: the preprint server for health sciences
26. Lam Isabel, Hallacli Erinc & Khurana Vikram. (2020). Proteome-Scale Mapping of Perturbed Proteostasis in Living Cells. Cold Spring Harbor perspectives in biology (2), a034124.